J Biomol NMR (2016) 66:1–7
DOI 10.1007/s10858-016-0053-x

COMMUNICATION

Towards interpretation of intermolecular paramagnetic relaxation enhancement outside the fast exchange limit

Alberto Ceccon[1] · G. Marius Clore[1] · Vitali Tugarinov[1]

Received: 11 July 2016 / Accepted: 12 August 2016 / Published online: 24 August 2016

Abstract In an exchanging system between major and minor species, the transverse paramagnetic relaxation enhancement rate observed on the resonances of the major species (Γ_2^{app}) is dependent upon the exchange regime between the species. Quantitative analysis of PRE data in such systems typically assumes that the overall exchange rate k_{ex} between the species is fast on the PRE time scale ($k_{ex} \gg \Gamma_2$). Recently, we have characterized the kinetics of binding of the model protein ubiquitin to large (LUV) and small (SUV) unilamellar lipid-based nanoparticles or liposomes (Ceccon A, Tugarinov V, Bax A, Clore GM (2016). J Am Chem Soc 138:5789–5792). Building upon these results and taking advantage of a strong paramagnetic agent with an isotropic g-tensor, Gd^{3+}, we were able to measure intermolecular methyl carbon and proton PREs between paramagnetically-tagged liposomes and ubiquitin. In the limit of fast exchange ($k_{ex} \gg \Gamma_2$) the ratio of the apparent proton to carbon methyl PREs, $(^1H_m–\Gamma_2^{app})/(^{13}C_m–\Gamma_2^{app})$, is equal to the square of the ratio of the gyromagnetic ratios of the two nuclei, $(\gamma_H/\gamma_C)^2$. However, outside the fast exchange regime, under intermediate exchange conditions (e.g. when Γ_2 is comparable in magnitude to k_{ex}) the $(^1H_m–\Gamma_2^{app})/(^{13}C_m–\Gamma_2^{app})$ ratio provides a reliable measure of the 'true' methyl PREs.

Keywords Paramagnetic relaxation enhancement · Chemical exchange · Ligand binding · Liposomes · Protein-nanoparticle interactions

Paramagnetic Relaxation Enhancement (PRE) is due to an increase in nuclear spin relaxation rates arising from interactions of nuclear spins with the spin of an unpaired electron. In structural biology applications, PRE measurements generally involve covalently attaching a tag containing a paramagnetic center with an isotropic g-tensor (such as a nitroxide free radical or an appropriate metal ion such as Mn^{2+} or Gd^{3+}) to the macromolecule of interest. The PRE is proportional to $<r^{-6}>$ (where r is the distance between the nucleus of interest and the unpaired electron), and, because of the large magnetic moment of the unpaired electron, the PRE effect is detectable for large nucleus-electron distances extending out to $\sim$20 Å for a nitroxide spin-label and $\sim$35 Å for Mn^{2+} and Gd^{3+}. As a result, the PRE has seen many applications in the study of folded and unfolded proteins, protein complexes and sparsely populated states (see (Clore and Iwahara 2009; Bashir et al. 2011; Luna et al. 2014; Anthis and Clore 2015; Clore 2015; Columbus and Kroncke 2015; Volkov 2015) for recent reviews).

In systems involving exchange between two or more species (e.g. alternate conformations, interaction between two binding partners) the experimentally observed PRE is mediated by inter-conversion between the states characterized by different PREs and, therefore, is dependent upon the kinetic parameters of the exchange process. This phenomenon has been exploited to detect and characterize

Electronic supplementary material The online version of this article (doi:10.1007/s10858-016-0053-x) contains supplementary material, which is available to authorized users.

✉ G. Marius Clore
mariusc@mail.nih.gov

✉ Vitali Tugarinov
vitali.tugarinov@nih.gov

[1] Laboratory of Chemical Physics, National Institute of Diabetes and Digestive and Kidney Diseases, National Institutes of Health, Bethesda, MD 20892-0520, USA

sparsely populated states where the distances between protons and the paramagnetic center are significantly shorter in the minor species than the major one (Iwahara and Clore 2006; Tang et al. 2006; Volkov et al. 2006). With a few notable exceptions, such as a recent study by Kay and co-workers which described the measurement of PREs in a system undergoing slow exchange using paramagnetic Chemical Exchange Saturation Transfer (para-CEST) (Sekhar et al. 2016), and the analyses of slow-to-intermediate exchange in paramagnetic systems (Bertini et al. 2000; Jensen et al. 2002; Hansen and Led 2003), analysis of intra- and intermolecular PREs in systems undergoing inter-conversion between two and more states typically assumes that the overall exchange rate k_{ex} between these states is fast on the timescale of the 'true' transverse PRE rate.

Here, we focus on intermolecular PRE measurements involving a binding equilibrium between the free (unliganded) state of a model protein, ubiquitin, and its complexes with paramagnetically-tagged large (LUV) and small (SUV) unilamellar lipid nanoparticles or liposomes. Recently, we characterized the kinetics of ubiquitin binding to both types of liposomes, as well as the global dynamics that ubiquitin undergoes on the surface of these nanoparticles (Ceccon et al. 2016). Combined analysis of life-time line broadening (ΔR_2) of ubiquitin resonances in the presence of LUV (diameter $\sim$ 100 nm) and SUV (diameter $\sim$ 27 nm) nanoparticles differing by an order of magnitude in their global effective correlation times, showed that the lifetime of bound ubiquitin was $\sim$20 μs, and that bound ubiquitin undergoes internal rotation on the microsecond time scale (correlation time $\sim$2 μs) about an axis perpendicular to the lipid surface (Ceccon et al. 2016). The data on the kinetics and dynamics of ubiquitin-liposome interactions do not, however, report directly on the location of the binding site on the surface of ubiquitin. To reliably map the interaction surface of ubiquitin with liposomes, we therefore supplemented the SUV and LUV ΔR_2 data with intermolecular PRE measurements using 10 % Gd^{3+}-tagged lipids in the liposome preparation (Ceccon et al. 2016). Although the rate of inter-conversion between free ubiquitin and its liposome-bound form is fast on the chemical shift time-scale, Gd^{3+}(total electron spin $S = 7/2$) is a very strong paramagnetic agent resulting in very high Γ_2 rates in the complex. Consequently, the magnitude of Γ_2 may become comparable to the exchange rate k_{ex}, placing such a system outside of the fast exchange limit on the PRE timescale, and as shown below, leading to a loss of information on the 'true' PRE. That is why the PREs were only interpreted qualitatively in our earlier study (Ceccon et al. 2016).

In this paper, we present the first attempt at a semi-quantitative treatment of intermolecular PRE data in the intermediate exchange regime where the 'true' PRE rate is similar in magnitude to the rate of inter-conversion between the two exchanging states. Building upon knowledge of the binding kinetics of ubiquitin-liposome interactions (Ceccon et al. 2016), we show that measurement of $^{13}C_{methyl}$ PREs ($^{13}C_m$–Γ_2^{app}) in conjunction with methyl proton PREs (^1H_m–Γ_2^{app}) provides valuable information on the 'true' methyl PREs (which, in favorable cases, can be recast in terms of distances to the paramagnetic center). This is achieved by comparing the observed (^1H_m–Γ_2^{app})/($^{13}C_m$–Γ_2^{app}) PRE ratio with the expected ratio in the absence of exchange or in the limit of fast exchange given by the square of the ratio of the gyromagnetic ratios of the two nuclei $(\gamma_H/\gamma_C)^2$.

In a system undergoing two-site exchange between the free state of a protein (observable state A) and its bound state ('dark' state B), the observed 'apparent' PRE, Γ_2^{app}, can be calculated as the difference between the decay of transverse magnetization in the paramagnetic and diamagnetic samples. In the absence of chemical shift differences between the two states, the evolution of magnetization in this system can be represented as the difference between two sets of simplified Bloch–McConnell equations (McConnell 1958; Helgstrand et al. 2000) (note that in our case the paramagnetic label is attached only to state B):

$$\frac{d}{dt}\begin{bmatrix} I^A \\ I^B \end{bmatrix} = -\left(\begin{bmatrix} R_2^A + k_{on}^{app} & -k_{off} \\ -k_{on}^{app} & R_2^B + \Gamma_2 + k_{on}^{app} \end{bmatrix} - \begin{bmatrix} R_2^A + k_{on}^{app} & -k_{off} \\ -k_{on}^{app} & R_2^B + k_{on}^{app} \end{bmatrix}\right)\begin{bmatrix} I^A \\ I^B \end{bmatrix} \quad (1)$$

where I^A and I^B are transverse magnetizations of states A and B, respectively, k_{on}^{app} is the apparent association rate constant, k_{off} is the dissociation rate constant, and R_2^A and R_2^B are the respective intrinsic transverse relaxation rates of the two states in the absence of exchange; the first and second terms on the right-hand side of Eq. 1 describe the evolution of magnetization in the paramagnetic and diamagnetic samples, respectively.

In practice, the decay of magnetization of the observable state A is always assumed to be single-exponential (a very good approximation for the parameters of exchange in this study). This allows us to express the observable PRE, Γ_2^{app}, as the difference between lifetime line broadening in the presence of liposomes ($\Delta R_2 = R_{2,obs}^A - R_2^A$) in the paramagnetic sample, ΔR_2^{para}, and in the diamagnetic sample, ΔR_2^{dia}: $\Gamma_2^{app} = \Delta R_2^{para} - \Delta R_2^{dia}$. The closed-form analytical solution for ΔR_2 (applicable for both dia- and paramagnetic samples), for initial conditions $\{I^A(0) = p_A;\ I^B(0) = 0\}$, where p_A is the equilibrium population of state A

($p_A = k_{off}/k_{ex}$, where $k_{ex} = k_{on}^{app} + k_{off}$), is given by (see Supplementary Information for details),

$$\Delta R_2 = (R_2^B - R_2^A + k_{off} + k_{on}^{app} - 2\eta)/2 \quad (2)$$

where $\eta = (1/2)\left[(R_2^B - R_2^A)^2 + (k_{off} + k_{on}^{app})^2 + 2(R_2^B - R_2^A)(k_{off} + k_{on}^{app})\right]^{1/2}$. Γ_2^{app} is then equal to,

$$\Gamma_2^{app} = \Gamma_2/2 + \eta_{dia} - \eta_{para} \quad (3)$$

where $\eta_{dia} = \eta$ as defined above, Eq. 2, and η_{para} is η with R_2^B substituted for $(R_2^B + \Gamma_2)$.

Figure 1a shows the theoretical dependence of the observed transverse ^{1}H PRE, ^{1}H-Γ_2^{app}, as a function of the 'true' PRE, ^{1}H-Γ_2, calculated numerically for the exchange parameters of the ubiquitin-LUV liposome interaction ($k_{on}^{app} = 50\ s^{-1}$; $k_{off} = 51{,}000\ s^{-1}$; $R_2^A = 10\ s^{-1}$; $R_2^B = 13{,}500\ s^{-1}$ (Ceccon et al. 2016)) using Eq. 1 (identical results are obtained using the analytical solution given by Eq. 3). If exchange is slow on the PRE time-scale (k_{ex} - Γ_2), Γ_2^{app} will asymptotically approach a limit given by,

$$\lim_{\Gamma_2 \to \infty} \Gamma_2^{app} = \left(k_{on}^{app} - k_{off} - (R_2^B - R_2^A) + 2\eta_{dia}\right)/2 \quad (4)$$

(shown by the dashed horizontal line in Fig. 1a). Note that the expression in Eq. 4 provides values slightly lower than k_{on}^{app} in this regime. Only when $R_2^B = R_2^A$ (*i.e.* the binding partners have similar molecular weights), $\lim_{\Gamma_2 \to \infty} \Gamma_2^{app} = k_{on}^{app}$ as is the case for ΔR_2 in the slow exchange regime (Fawzi et al. 2010). Conversely, in the limit of fast exchange on both the PRE ($k_{ex} \gg \Gamma_2$) and intrinsic transverse relaxation rate ($k_{ex} \gg R_2^B$) time scales, Γ_2^{app} approaches a limiting value of $p_B\Gamma_2$ (cf. Eq. 3), where p_B is the population of the bound state ($p_B = 1 - p_A = k_{on}^{app}/k_{ex}$). Clearly, the sensitivity of the measured Γ_2^{app} to the 'true' Γ_2 decreases as Γ_2 increases: in the limit of very slow exchange on the PRE time-scale ($k_{ex} \ll \Gamma_2$), Γ_2^{app} is not a good reporter of Γ_2 as its value reaches the limit defined by Eq. 4 (Fig. 1a, dashed red line). The measured Γ_2^{app} values are linearly dependent on the value of k_{on}^{app} (and the population of the bound state, p_B). Thus, for the same value of Γ_2, higher values of Γ_2^{app} are predicted for SUV liposomes used in this study ($k_{on}^{app} \sim 200\ s^{-1}$) as illustrated in the inset to Fig. 1a.

Exploiting the strength of the Gd^{3+} paramagnetic probe, we supplement ^{1}H PREs (routinely acquired in structural studies of paramagnetically labelled macromolecules, as the PRE scales with the square of the nuclear gyromagnetic ratio and is, therefore, largest for ^{1}H nuclei), with ^{13}C PRE measurements. In methyl groups, combined analysis of these two sets of PRE data (^1H_m– and $^{13}C_m$–PRE) is possible. The theoretical ratio of ^{1}H to ^{13}C Γ_2^{app}, $R = (^1H_m\text{–}\Gamma_2^{app})/(^{13}C_m\text{–}\Gamma_2^{app})$, calculated as a function of Γ_2 using Eq. 1 for ubiquitin-liposome interactions with ^{13}C–Γ_2 set to $(\gamma_C/\gamma_H)^2(^1H\text{–}\Gamma_2)$, is shown in Fig. 1b. In the limit of fast exchange ($k_{ex} \gg \Gamma_2$), the ratio R is expected to be equal to the square of the ratio of the gyromagnetic ratios of the two nuclei, $(\gamma_H/\gamma_C)^2$. Beyond this limit, however, R can adopt values significantly lower than $(\gamma_H/\gamma_C)^2$. For the ubiquitin-liposome system considered here, R is practically independent of k_{on}^{app}, because even large changes in k_{on}^{app} do not affect the exchange regime (k_{ex}) to any significant extent in a system with highly skewed populations of the interconverting species ($p_A \gg p_B$, and $k_{on}^{app} \ll k_{off} \sim k_{ex}$). Further, the dependence of R on Γ_2 in Fig. 1b is only marginally sensitive to the exact values of the transverse relaxation rates in the bound state, R_2^B, of either methyl proton

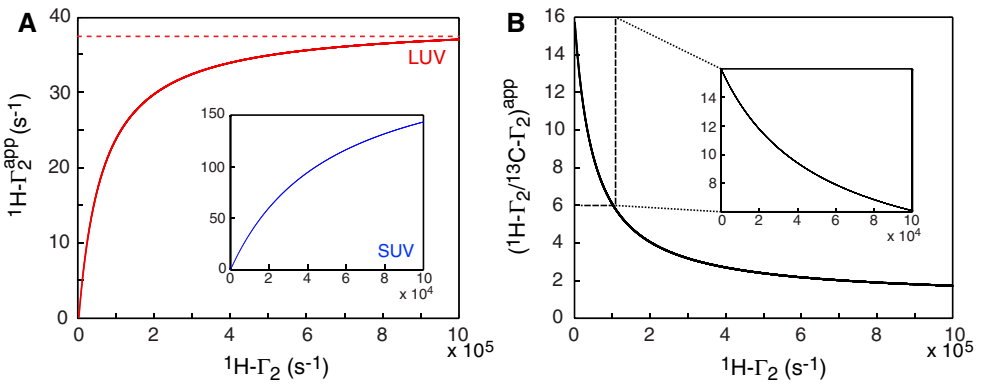

Fig. 1 Theoretical dependence of the (**A**) observed ^{1}H-Γ_2^{app} rate and (**B**) $(^1H\text{-}\Gamma_2/^{13}C\text{-}\Gamma_2)^{app}$ ratio on the 'true' ^{1}H-Γ_2 rate. *Curves* are calculated by solving Eq. 1 numerically using the parameters of the ubiquitin-LUV liposome system: $k_{on}^{app} = 50\ s^{-1}$; $k_{off} = 51{,}000\ s^{-1}$; $R_2^A = 10\ s^{-1}$; $R_2^B = 13{,}500\ s^{-1}$ (Ceccon et al. 2016). The asymptotic limit calculated using Eq. 4 is indicated by the *dashed red line*. The *inset* in panel A shows the same *plot* calculated for the ubiquitin-SUV liposome system:$k_{on}^{app} = 225\ s^{-1}$; $k_{off} = 51{,}000\ s^{-1}$; $R_2^A = 10\ s^{-1}$; $R_2^B = 1500\ s^{-1}$ (Ceccon et al. 2016). Note that LUVs and SUV particles have diameters of ~100 and 27 nm, respectively (Ceccon et al. 2016). The same color-coding is used throughout the paper: LUV, *red*; SUV, *blue*. The *inset* in panel B shows an expanded plot of the region $6 \le (^1H\text{–}\Gamma_2/^{13}C\text{–}\Gamma_2)^{app} \le 16$, corresponding to the values observed experimentally

(^1H_m–R_2^B) or methyl carbon ($^{13}C_m$–R_2^B), providing the magnitude of these two relaxation rates are not dramatically different. However, even for ^1H_m–R_2^B values that are $< \sim$ fourfold larger than $^{13}C_m$–R_2^B, variations in the ratio R remain very small. Conversely, as in exchanging systems with highly skewed populations of the interconverting species, the exchange regime is determined primarily by the dissociation rate constant, k_{off}, and hence the ratio R is very sensitive to the value of k_{off} (see Supporting Information, Fig. S1). Comparison of the experimentally measured R value with the limiting value ($\gamma_H^2/\gamma_C^2 = 15.81$) thus serves as a robust measure of the 'true' PRE in both LUV- and SUV-ubiquitin complexes which are characterized by the same value of k_{off} (Ceccon et al. 2016).

Paramagnetically tagged, negatively charged liposomes were obtained by addition of the gadolinium salt of 1,2-distearoyl-sn-glycero-3-phosphoethanolamine-N-diethylenetriamine pentaacetic acid (PE-DTPA-Gd^{3+}) at 10 % mol/mol concentration to LUV/SUV liposome formulations. LUV liposomes were prepared as described previously (Ceccon et al. 2016), while the extrusion step was omitted and replaced by sonication in the preparation of SUV particles (see Supplementary Information). Figure 2A and B show the ^1H_m–Γ_2^{app} and $^{13}C_m$–Γ_2^{app} profiles, respectively, measured on ubiquitin in the presence of LUV liposomes (1:2 ubiquitin:lipid molar ratio), while Fig. 2C and D show the corresponding data obtained with SUV particles (1:0.5 molar ratio). The experimental details pertaining to liposome preparation and NMR acquisition of ^1H_N, ^1H_m, and $^{13}C_m$ PRE data are described in the Supplementary Information. As in our previous study (Ceccon et al. 2016), where we concentrated on amide (^1H_N) and methyl (^1H_m) proton PREs only, a uniform background PRE is observed in the plots shown in Fig. 2A-D, equal to $\sim$27 and 2 s^{-1} for ^1H_m and $^{13}C_m$, respectively, in the ubiquitin-LUV system, and to $\sim$7 and 0.5 s^{-1} for ^1H_m and $^{13}C_m$, respectively, in ubiquitin-SUV system. The background arises from the magnetic field generated by the paramagnetic tags attached to the liposome nanoparticles (note that a relatively high concentration of Gd^{3+} tags is used)—an effect similar to the blood-oxygen-level dependent (BOLD) effect in functional MRI (Ogawa et al. 1990). Unlike the PRE effect itself, the background scales approximately with the concentration of (Gd^{3+}-tagged) lipids, *i.e.* it is dependent on the total amount of gadolinium ions in solution. As the background stems from a relaxation mechanism that is different from that of the conventional PRE, it has to be subtracted from the measured ^1H_m–Γ_2^{app} and $^{13}C_m$–Γ_2^{app} values before any meaningful analysis can be undertaken. As in our previous study of ubiquitin-liposome interactions (Ceccon et al. 2016), as a 'negative control', we conducted PRE measurements of (1) ubiquitin in the presence of zwitterionic (POPC) liposomes,

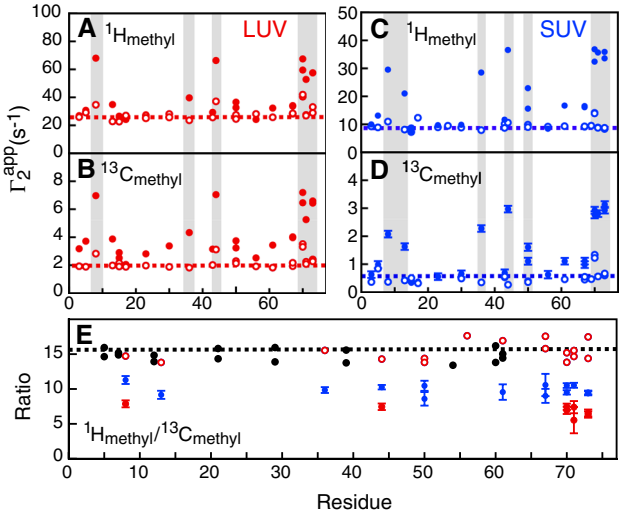

Fig. 2 Experimental ^1H_m–Γ_2^{app} and $^{13}C_m$–Γ_2^{app} values and (^1H_m–Γ_2^{app})/($^{13}C_m$–Γ_2^{app}) ratios measured for ubiquitin in the presence of Gd^{3+}–tagged negatively charged liposomes. **A** and **B** ^1H and ^{13}C methyl PREs, respectively, for ubiquitin in the presence of negatively charged POPG LUV liposomes (*filled red circles*; 1:2 ubiquitin:lipid molar ratio). **C** and **D** ^1H and ^{13}C methyl PREs, respectively, for ubiquitin in the presence of negatively charged POPG SUV liposomes (*filled blue circles*; 1:0.5 ubiquitin:lipid molar ratio). The *dashed horizontal lines* in panels (**A**–**D**) show the approximate level of the PRE background (see text). Control PRE values obtained for the ^1H and ^{13}C methyls of ubiquitin in the presence of zwitterionic POPC liposomes are shown with *open red* (LUV) and *blue* (SUV) *circles*. The regions in proximity to the ubiquitin-liposome binding surface are highlighted in *grey*. **E** Experimental ratios of ^1H to ^{13}C methyl PREs, $R = (^1H_m–\Gamma_2^{app})/(^{13}C_m–\Gamma_2^{app})$, obtained in the presence of negatively charged LUV (*filled red circles*) and SUV (*filled blue circles*) particles. The values of R obtained for ubiquitin in the presence of zwiterionic POPC liposomes are shown with *open red circles*, while the values of R measured for GB1 in the presence of negatively charged POPG liposomes are shown with *filled black circles*. The theoretical ratio of $(\gamma_H/\gamma_C)^2 = 15.81$, predicted in the absence of binding, is displayed by the horizontal *dashed line*

and (2) the negatively charged protein GB1 (net charge −4 at pH = 6.8) with negatively charged POPG liposomes. Both measurements yield PREs essentially in the background (shown with open red and blue circles for LUV and SUV, respectively, in Fig. 2A-D) indicating that the interactions of ubiquitin with negatively charged liposome nanoparticles are specific and require a positively charged patch on the surface of ubiquitin. We note that after background subtraction is carried out, the PREs in the presence of negatively charged POPG LUVs remain higher by a factor of $\sim$2 on average (taken over all methyls in ubiquitin with ^1H_m and $^{13}C_m$ PREs above the background) compared to those for ubiquitin-POPG SUVs despite the fact that k_{on}^{app}(and, hence, the population of the bound state) for the ubiquitin-SUV interaction under the conditions of this study (1:0.5 protein:lipid ratio) is $\sim$fourfold higher than that for the ubiquitin-LUV interaction.

This observation can be explained only if the 'true' PRE Γ_2 is significantly lower for ubiquitin-SUV than ubiquitin-LUV complexes, as we show below is indeed the case.

Figure 2E plots the ratios R of methyl $^{1}H_m$ to $^{13}C_m$ PREs obtained for ILV methyls in the ubiquitin-LUV (red circles) and ubiquitin-SUV (blue circles) systems after background subtraction. The values of R obtained for ubiquitin in the presence of zwitterionic POPC liposomes and those measured for GB1 in the presence of negatively charged POPG liposomes cluster around the theoretical ratio of $(\gamma_H/\gamma_C)^2 = 15.81$ predicted in the absence of binding (Fig. 2e), while for ubiquitin in the presence of negatively charged POPG LUV- or SUV-liposomes, the average ratio R is 6.9 and 9.8 for LUVs and SUVs, respectively. For the subset of methyl groups, where PREs could be measured for both LUV and SUV liposomes, the values of R are systematically higher in the presence of SUV particles indicating that the exchange regime on the PRE timescale is somewhat different for the interactions with SUV and LUV particles. This can only occur if Γ_2 is significantly lower in the SUV case.

The effective global correlation times (derived from the rotational diffusion correlation times and the rate of exchange) for ubiquitin-SUV and ubiquitin-LUV complexes obtained from relaxation analysis are $\sim$1.6 and $\sim$16 μs, respectively (Ceccon et al. 2016). For these correlation times, one would expect that at high static magnetic fields the PRE would be dominated by the Curie spin relaxation mechanism. The contribution of this mechanism to PRE can be easily ascertained by PRE measurements at different spectrometer fields, as Curie spin relaxation is dependent on the square of the magnetic field. This expectation, however, is not borne out by our experimental data. While the PRE background is dependent upon the spectrometer field (Fig. 3a) as expected from previous reports on the field dependence of the BOLD effect (Gati et al. 1997; Triantafyllou et al. 2011), after subtraction of the background the $^{1}H^{N}$ PRE values measured for ubiquitin in the presence of liposomes are practically field-independent as shown in Fig. 3b, c for LUVs and SUVs, respectively. Very high global correlation times for ubiquitin-LUV and –SUV complexes can be only reconciled with the observed absence of Curie spin relaxation if the electronic correlation time for liposome-attached Gd^{3+}–DTPA is very high (in the low microsecond range).

In the limit of a very high correlation time $\tau_{c,eff}$, the electronic longitudinal relaxation time (T_{1e}) of Gd^{3+} is practically independent of $\tau_{c,eff}$ (Benmelouka et al. 2007). T_{1e}, however, does depend on the strength of the static (spectrometer) magnetic field and the vibrational correlation time, τ_v, which, in turn, is a function of (i) the type of metal coordination cage, (ii) temperature, and, most importantly, (iii) the chemistry of cage attachment to the surface of a nanoparticle. For example, very low vibrational times ($\sim$1 ps) were reported for free Gd^{3+}–DTPA (Benmelouka et al. 2007), while values of 20–24 ps have been reported by Bertini and co-workers (Alhaique et al. 2002; Bertini et al. 2004) for liposome-attached PE-DTPA with a 14–carbon long lipid chain at 298 K–the closest analogue to our study, where an 18-carbon lipid chain is used. Using the Solomon-Bloembergen-Morgan (SBM) equations for electron longitudinal relaxation (Benmelouka et al. 2007) with $\tau_v = 20$ ps, we calculate a value of 2.7 μs for the Gd^{3+} T_{1e} (at 700 MHz and 298 K). Using this value for T_{1e} in the Solomon-Bloembergen equations for the PRE (Clore and Iwahara 2009) due to nuclear-electron dipole–dipole and Curie-spin relaxation mechanisms, we estimate that the contribution of Curie-spin relaxation to the total PRE is only $\sim$12 % for LUV complexes and less than 2 % for SUV ones. Even for LUV liposomes, this contribution is relatively small, and would translate to a slope of $\sim$ 1.06 in Fig. 3b. The fact that even smaller ratios of PREs at two spectrometer fields are observed in the plot of Fig. 3b may be the result of inaccuracies in background subtraction (note that the bulk of the PRE field dependence is thus subtracted with the background which shows significant dependence on the spectrometer field, Fig. 3a).

We note that because the resulting value of the Gd^{3+} T_{1e} (2.7 μs) exceeds the value of $\tau_{c,eff}$ for the ubiquitin-SUV complex (1.6 μs), even PREs due to nucleus-electron dipolar interactions effectively become dependent of the value of the global correlation time. That is why the calculation of the 'true' PRE Γ_2 for ubiquitin-SUV complexes (for an arbitrary distance between the nucleus and unpaired electrons of Gd^{3+}) results in $\sim$2.3-fold lower values than for ubiquitin-LUV complexes ($\tau_{c,eff} \sim 16$ μs), leading to smaller apparent PRE values (*cf.* Fig. 2a vs 2c, and Fig. 2b vs 2d) and systematically higher ^{1}H to ^{13}C methyl PRE ratios for ubiquitin-SUV as compared to ubiquitin-LUV complexes (Fig. 2e). The values of the ^{1}H to ^{13}C methyl PRE ratios obtained for individual methyl groups of ubiquitin in the presence of LUV and SUV liposomes are: 7.9 and 11.3, respectively, for Leu8-δ1; 7.5 and 10.3 for Ile44-δ1; 7.4 and 10.5 for Val70-δ1; 6.9 and 9.5 for Val70-δ2; 7.4 and 10.5 for Leu71-δ1; 6.5 and 9.5 for Leu73-δ1; and 6.3 and 9.4 for Leu73-δ2.

The complexity of the paramagnetic labeling pattern involving multiple Gd^{3+} tags on the surface of liposomes, as well as the complicated dynamics of the ubiquitin liposome-bound state (Ceccon et al. 2016) preclude direct interpretation of the PRE data in terms of distances between the relaxation-enhanced nuclei and the unpaired electrons of the paramagnetic probe. However, using the theoretical curves shown in Fig. 1b, we can reliably estimate the 'true' ^{1}H methyl PRE values for the ubiquitin-liposome complexes from the ^{1}H to ^{13}C methyl PRE ratios

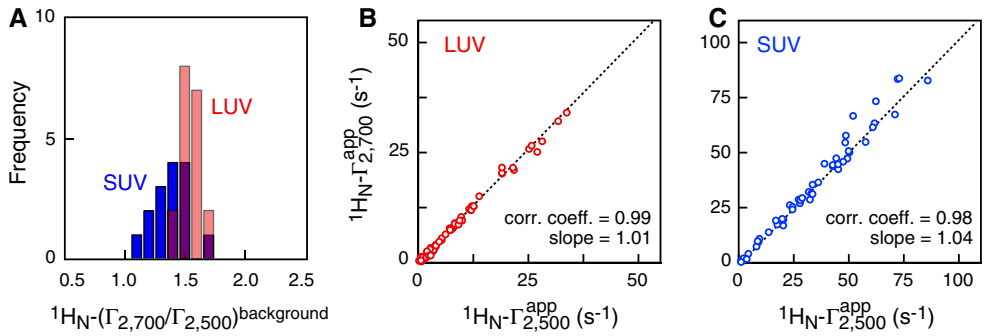

Fig. 3 Spectrometer field dependence of ^1H_N PREs measured on ubiquitin in the presence of LUVs and SUVs. **A** Histograms of ratios of ^1H_N background PREs obtained at 700 and 500 MHz for LUV (*red bars*) and SUV (*blue bars*) nanoparticles. Correlation *plots* of apparent ^1H_N-Γ_2 values obtained at 700 (*y*-axis) and 500 (*x*-axis) MHz spectrometer fields after the subtraction of the PRE background for (**B**) ubiquitin-LUV (*red open circles*) and (**C**) ubiquitin-SUV (*blue open circles*) systems

(*R*). The calculated 'true' ^1H_m–Γ_2 values range from ~60,000 s^{-1} ($R = 7.9$ for Leu8-δ1) to ~80,000 s^{-1} ($R = 6.3$ for Leu73-δ1) for LUV complexes, and from ~30,000 s^{-1} ($R = 11.3$ for Leu8-δ1) to ~ 40,000 s^{-1} ($R = 9.4$ for Leu73-δ1) for SUV complexes. The estimated values of Γ_2 for LUV and SUV liposomes thus lie at opposing ends of the exchange rate (k_{ex} ~ 50,000 s^{-1}). It is clear, however, that in both instances the calculated Γ_2 values are not in the fast exchange limit usually assumed to be applicable in studies of intermolecular PREs. Both LUV and SUV calculated Γ_2 values correspond to distances of 18–19 Å between nuclear probes and the electrons of the Gd^{3+} tag. For a subset of methyl groups in ubiquitin, PREs (specifically for Ile13-δ1, $R = 9.2$; Ile36-δ1, $R = 9.9$; Leu50-δ1, $R = 8.6$; Leu50-δ2, $R = 10.5$; Ile61-δ1, $R = 9.6$; Leu67-δ1, $R = 10.6$; and Leu67-δ1, $R = 9.1$) could be measured only in the presence of SUV liposomes due to the larger value of k_{on}^{app} and concomitant larger population of the bound state.

The property of the ^1H to ^{13}C methyl PRE ratio, *R*, that is particularly attractive lies in its virtual independence on the value of the binding on-rate, k_{on}^{app}, and, hence, the population of the bound state (at least, for the ubiquitin-liposome interactions in question, where the populations of the exchanging species are highly skewed, $p_A \gg p_B$, and $k_{on}^{app} \ll k_{off} \sim k_{ex}$). As a consequence, for particles covering a wide range of sizes, the ratio *R* is not sensitive to the exact quantities of liposomes added, which may be difficult to control experimentally. Therefore, the determination of Γ_2 via analysis of the ratio *R* (cf. Figure 1b) is less error-prone than a direct estimation of Γ_2 from ^1H_m–Γ_2^{app} or $^1H^N$–$\Gamma_2{}^{app}$ values (Fig. 1a).

In conclusion, using the strong paramagnetic agent Gd^{3+} we were able to measure methyl carbon PREs, $^{13}C_m$–Γ_2^{app}, in conjunction with methyl proton PREs, ^1H_m–Γ_2^{app}, for the model protein ubiquitin binding to LUV and SUV liposome nanoparticles. We show that the ratio of these PREs, $R = (^1H_m\text{–}\Gamma_2^{app})/(^{13}C_m\text{–}\Gamma_2^{app})$, which in the limit of fast exchange is equal to the square of the ratio of gyromagnetic ratios γ of the two nuclei, $(\gamma_H/\gamma_C)^2$, serves as a robust measure of the 'true' methyl PRE in the complex, Γ_2, in the intermediate exchange regime where Γ_2 is comparable in magnitude to the rate of exchange k_{ex}.

Acknowledgments We thank Dr. Attila Szabo for useful discussions. This work was supported by funds from the Intramural Program of the NIH, NIDDK, and the Intramural AIDS Targeted Antiviral Program of the Office of the Director of the NIH (to G.M.C.).

References

Alhaique F, Bertini I, Fragai M, Carafa M, Luchinat C et al (2002) Solvent ^1H NMRD study of biotinylated paramagnetic liposomes containing Gd-bis-SDA-DTPA or Gd-DMPE-DTPA. Inorg Chim Acta 331:151–157

Anthis NJ, Clore GM (2015) Visualizing transient dark states by NMR spectroscopy. Q Rev Biophys 48:35–116

Bashir Q, Scanu S, Ubbink M (2011) Dynamics in electron transfer protein complexes. FEBS J 278:1391–1400

Benmelouka M, Borel A, Moriggi L, Helm L, Merbach AE (2007) Design of Gd(III)-based magnetic resonance imaging contrast agents: static and transient zero-field splitting contributions to the electronic relaxation and their impact on relaxivity. J Phys Chem B 111:832–840

Bertini I, Fernandez CO, Karlsson BG, Leckner J et al (2000) Structural information through NMR hyperfine shifts in blue copper proteins. J Am Chem Soc 122:2701–3707

Bertini I, Bianchini F, Calorini L, Colagrande S, Fragai M et al (2004) Persistent contrast enhancement by sterically stabilized paramagnetic liposomes in murine melanoma. Magn Reson Med 52:669–672

Ceccon A, Tugarinov V, Bax A, Clore GM (2016) Global dynamics and exchange kinetics of a protein on the surface of nanoparticles revealed by relaxation-based solution NMR spectroscopy. J Am Chem Soc 138:5789–5792

Clore GM (2015) Practical aspects of paramagnetic relaxation enhancement in biological macromolecules. Methods Enzymol 564:485–497

Clore GM, Iwahara J (2009) Theory, practice, and applications of paramagnetic relaxation enhancement for the characterization of transient low-population states of biological macromolecules and their complexes. Chem Rev 109:4108–4139

Columbus L, Kroncke B (2015) Solution NMR structure determination of polytopic α-helical membrane proteins: a guide to spin label paramagnetic relaxation enhancement restraints. Methods Enzymol 557:329–348

Fawzi NL, Ying J, Torchia DA, Clore GM (2010) Kinetics of amyloid β monomer-to-oligomer exchange by NMR relaxation. J Am Chem Soc 132:9948–9951

Gati JS, Menon RS, Ugurbil K, Rutt BK (1997) Experimental determination of the BOLD field strength dependence in vessels and tissue. Magn Reson Med 38:296–302

Hansen DF, Led JJ (2003) Inplications of using approximate Bloch-McConnell equations in NMR analyses of chemically exchanging systems: application to the electron self-exchange of plastocyanin. J Magn Reson 163:215–227

Helgstrand M, Härd T, Allard P (2000) Simulations of NMR pulse sequences during equilibrium and non-equilibrium chemical exchange. J Biomol NMR 18:49–63

Iwahara J, Clore GM (2006) Detecting transient intermediates in macromolecular binding by paramagnetic NMR. Nature 440:1227–1230

Jensen MR, Hansen DF, Led JJ (2002) A general method for determining electron self-exchange rates of blue copper proteins by longitudinal NMR relaxation. J Am Chem Soc 124:296–304

Luna RE, Akabayov SR, Ziarek JJ, Wagner G (2014) Examining weak protein-protein interactions in start codon recognition via NMR spectroscopy. FEBS J 281:1965–1973

McConnell HM (1958) Reaction rates by nuclear magnetic resonance. J Chem Phys 28:430–431

Ogawa S, Lee TM, Kay AR, Tank DW (1990) Brain magnetic resonance imaging with contrast dependent on blood oxygenation. Proc Natl Acad Sci USA 87:9868–9872

Sekhar A, Rosenzweig R, Bouvignies G, Kay LE (2016) Hsp70 biases the folding pathways of client proteins. Proc Natl Acad Sci USA 113:E2794–E2801

Tang C, Iwahara J, Clore GM (2006) Visualization of transient encounter complexes in protein-protein association. Nature 444:383–386

Triantafyllou C, Wald LL, Hoge RD (2011) Echo-Time and field strength dependence of BOLD reactivity in Veins and Parenchyma using flow-normalized hypercapnic manipulation. PLoS ONE 6:e24519

Volkov AN (2015) Structure and function of transient encounters of redox proteins. Acc Chem Res 48:3036–3043

Volkov AN, Worrall JA, Holtzmann E, Ubbink M (2006) Solution structure and dynamics of the complex between cytochrome c and cytochrome c peroxidase determined by paramagnetic NMR. Proc Natl Acad Sci USA 103:18945–18950